J. Fluid Mech. (1987), *vol.* 178, *pp.* 243–256
Printed in Great Britain

Stokes flow down a wall into an infinite pool

By ERIK B. HANSEN
Laboratory of Applied Mathematical Physics, Technical University of Denmark, DK-2800, Lyngby, Denmark

(Received 21 January 1986 and in revised form 5 September 1986)

The two-dimensional flow of a thin film down a vertical or tilted plane wall into an infinite pool is studied in the Stokes approximation, the principal aim being to determine the shape of the fluid surface. Results are obtained for fluids with or without surface tension. Earlier results by Ruschak, that the surface tension gives rise to thickness variation of the film, are confirmed. For small or vanishing surface tension a dip of the pool surface is found to exist close to the wall. The case of a wall moving downwards is also considered.

1. Introduction

Consider a film of a Newtonian fluid flowing steadily down a plane wall into a large pool. The wall may be vertical or tilted and it may be at rest or moving upwards or downwards in its own plane. In this paper we study such a flow in the Stokes approximation. Our principal aim is to determine the shape of the free surface of the fluid.

If the wall is moving upwards so fast that fluid is being withdrawn from the pool rather than flowing into it, the flow is called a coating flow because of its application in industrial coating processes. A review of work on this and other types of coating flows has recently been given by Ruschak (1985). Here we are interested in phenomena which occur if the wall is at rest or moving downwards. So we shall primarily consider these cases.

It has been observed by Cook & Clark (1973) and others that when a thin film flows down a wall into a pool a system of waves may exist on its surface just above the region where the film merges with the pool. The waves were investigated theoretically by Ruschak (1978), who was able to explain them as being caused by pressure gradients set up by the surface-tension forces. In his analysis Ruschak divided the flow field into two regions, the film and the pool, and used different approximations in them. In the film he used lubrication theory to derive an ordinary differential equation for the film thickness. In the pool he neglected the dynamic forces so that the surface shape was governed by the differential equation for a hydrostatic meniscus with surface tension. Assuming that an intermediate region exists in which both approximations apply, he determined an approximation to the complete fluid surface. When solving his equations numerically, Ruschak found that a system of waves with the amplitude rapidly diminishing in the upward direction existed on the film. A plot presented in the paper shows the first of the waves and it is seen that at the trough just above the pool surface the film is considerably thinner than at infinity. Another plot shows that the minimum thickness decreases and the maximum thickness (which is assumed at the crest of the first wave) increases, as the surface tension is increased, a fact which supports Ruschak's explanation of the phenomenon, of which we shall give an account later.

More recently Wilson & Jones (1983) have studied the wave system using the method of matched asymptotic expansions to solve Ruschak's differential equation for the film thickness in the limit of large surface tension (i.e. $\beta \to \infty$, in the notation introduced below). They found that in order that the film can merge with a hydrostatic membrane its thickness must first undergo an indefinite large number of nonlinear 'leaps', the sizes of which, however, are such that only one or two waves should be expected to be seen in experiments and numerical solutions. Their analysis also showed that an estimate of the minimum film thickness, which Ruschak had given and confirmed by his numerical results, was asymptotically correct. Finally, they extended the investigation to the case of a downward moving wall in order to see if such a motion would cause a dip in the pool surface or other changes which might indicate the onset of air entrainment observed to occur in practice in such situations. However, in the limit which they considered, they found no such behaviour.

The present investigation differs from those of Ruschak and Wilson & Jones in that, apart from the Stokes flow approximation, no physical approximations are introduced in the analysis. Our numerical results correspond to values of the surface tension which are considerably smaller than those considered by Ruschak. They support his explanation of the thinning of the film and agree as closely as might be expected with Wilson & Jones' asymptotic theory. Like Wilson & Jones we extend our analysis to moving walls and find that a dip in the surface does indeed occur under certain circumstances. Finally we extend the investigation to non-vertical walls. Our method of solution is based on an integral formula for the stream function and an integral equation for the fluid velocity in the surface. A brief account of our method, but with no numerical results included, has previously been given by Hansen (1985). Kelmanson (1983) has solved other Stokes-flow free-surface problems using an integral-equation method which, however, is different from the one used here.

2. The problem

In our analysis we use an (x, y)-coordinate system of which the x-axis is on the wall with positive direction towards the pool as indicated in figure 1. The origin is at the intersection between the wall and the horizontal asymptote of the pool surface which, we suppose, extends to infinity. The angle between the wall and the vertical is denoted by ϑ_0. The wall moves in its own plane with a velocity u towards the pool. Then the flux, c, into the pool per unit length across the wall is positive if u is larger than a certain negative value.

We assume the fluid to be Newtonian and incompressible with dynamic viscosity μ, density ρ, and surface tension constant σ, and that the absolute values of u and c are small enough to make the Stokes approximation applicable throughout the entire fluid region. Then the pressure, p, and the stream function, ψ, which is defined so that the velocity is equal to $(\psi_y, -\psi_x)$, satisfy the equations

$$\frac{\partial p}{\partial x} = \mu \frac{\partial \Delta \psi}{\partial y} + \rho g \cos \vartheta_0, \quad \frac{\partial p}{\partial y} = -\mu \frac{\partial \Delta \psi}{\partial x} - \rho g \sin \vartheta_0, \tag{2.1}$$

where g is the acceleration of gravity. We satisfy the no-slip boundary condition by requiring that $\psi = -c$ and $\psi_y = u$ on the wall. Then $\psi = 0$ in the surface. We put the external pressure equal to zero. Then the boundary conditions that the shear stress vanishes and the normal stress balances the surface-tension force per unit area also hold in the surface. The surface-tension force per unit area is equal to $\sigma\kappa$, where

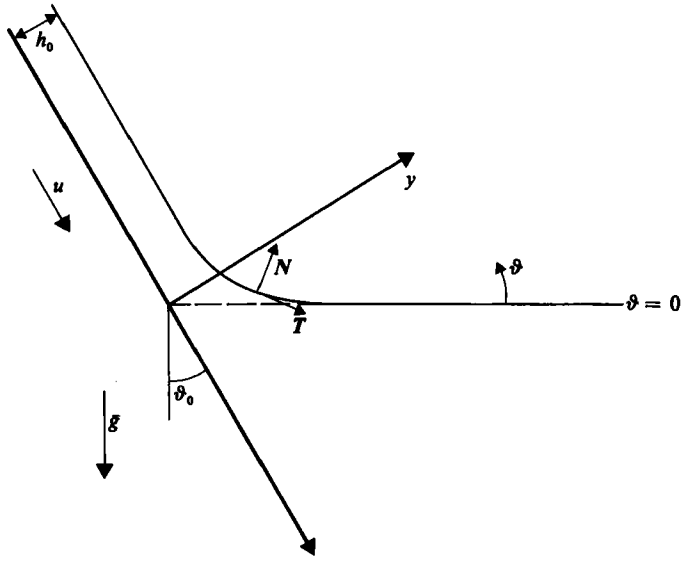

FIGURE 1. A film of thickness h_0 is flowing down a wall into an infinite pool. The wall is moving downwards with velocity u.

κ is the curvature of the intersection, C, between the surface and the (x, y)-plane. At a point on C with unit tangent and normal vectors T and N respectively, the two stress conditions may be expressed as

$$\Delta\psi = 2\frac{\partial^2\psi}{\partial T^2}, \quad p + 2\mu\frac{\partial^2\psi}{\partial T\,\partial N} + \sigma\kappa = 0. \tag{2.2}$$

The Cartesian derivatives $\partial^2/\partial T^2$ and $\partial^2/\partial T\,\partial N$ are expressed in terms of derivatives with respect to the arc length s and in the normal direction as

$$\frac{\partial^2}{\partial T^2} = \frac{\partial^2}{\partial s^2} - \kappa\frac{\partial}{\partial N}, \quad \frac{\partial^2}{\partial T\,\partial N} = \frac{\partial}{\partial s}\left(\frac{\partial}{\partial N}\right) + \kappa\frac{\partial}{\partial s}. \tag{2.3}$$

Therefore, and because $\psi = 0$ in the surface, the two conditions in (2.2) can also be written

$$\Delta\psi + 2\kappa\frac{\partial\psi}{\partial N} = 0, \quad p + 2\mu\frac{\partial}{\partial s}\left(\frac{\partial\psi}{\partial N}\right) + \sigma\kappa = 0. \tag{2.4}$$

For $x \to -\infty$ the film thickness approaches a constant value h_0, say, and the fluid velocity becomes parallel to the wall. It therefore follows from (2.1) and the boundary conditions that the flux can be expressed as

$$c = \psi_0 + h_0 u \quad \text{where } \psi_0 = \frac{\rho g h_0^3 \cos\vartheta_0}{3\mu}. \tag{2.5}$$

We write the problem defined above in a non-dimensional form by measuring all lengths in units of h_0, ψ in units of ψ_0, and p in units of the quantity $p_0 = \mu\psi_0/h_0^2$. The problem is then expressed by the following equations and conditions in which the non-dimensional variables are denoted by the same symbols as the corresponding dimensional ones:

$$\frac{\partial p}{\partial x} = \frac{\partial\Delta\psi}{\partial y} + 3, \quad \frac{\partial p}{\partial y} = -\frac{\partial\Delta\psi}{\partial x} - 3\alpha, \tag{2.6}$$

in the fluid region,

$$\psi = -1-\gamma, \quad \frac{\partial \psi}{\partial y} = \gamma, \tag{2.7}$$

on the wall ($y = 0$), and

$$\psi = 0, \quad \Delta\psi + 2\kappa \frac{\partial \psi}{\partial N} = 0, \quad p + 2\frac{\partial}{\partial s}\left(\frac{\partial \psi}{\partial N}\right) + \beta\kappa = 0, \tag{2.8}$$

in the surface. The parameters in (2.6), (2.7), and (2.8) are

$$\alpha = \tan\vartheta_0, \quad \beta = \frac{3\sigma}{\rho g h_0^2 \cos\vartheta_0}, \quad \gamma = \frac{h_0 u}{\psi_0}. \tag{2.9}$$

It follows from (2.6) that ψ is biharmonic.

In the non-dimensional coordinates the fluid surface approaches $y = 1$ and $\psi_{-\infty} = -\frac{1}{2}y^3 + \frac{3}{2}y^2 + \gamma y - \gamma - 1$ is an asymptotic representation of the stream function as $x \to -\infty$. Thus, the surface velocity approaches the value $v_{-\infty} = \gamma + \frac{3}{2}$ as $x \to -\infty$. As boundary condition at infinity in the pool it is sufficient to require that the velocity remains finite, that is that $\psi = O(r)$.

3. The method of solution

We determine the shape of the fluid surface and the flow velocity in the surface from an integral-equation formulation of our problem.

Since the stream function, ψ, is biharmonic its value at an arbitrary point, $\boldsymbol{r}_0$, in the fluid region can be expressed as a contour integral,

$$\psi(\boldsymbol{r}_0) = \int_{\partial\Omega} \left[\frac{\partial \Delta\psi}{\partial N} G - \Delta\psi \frac{\partial G}{\partial N} + \frac{\partial \psi}{\partial N}\Delta G - \psi \frac{\partial \Delta G}{\partial N}\right] \mathrm{d}s. \tag{3.1}$$

Here $\partial\Omega$ is an arbitrary closed curve in the fluid region encircling $\boldsymbol{r}_0$, $G = G(\boldsymbol{r}, \boldsymbol{r}_0)$ is a fundamental solution to the biharmonic equation, and $\partial/\partial N$ denotes differentiation in the outward normal direction to $\partial\Omega$. Formula (3.1) is derived by straightforward applications of Green's second identity. We use (3.1) with $\partial\Omega$ consisting of the x-axis and the intersection, C, between the surface and the (x, y)-plane, $\partial\Omega$ being closed by a line section $x = -x_- < 0$ and a circular arc $r = r_+$ in the pool. For G we choose the function

$$G(\boldsymbol{r}, \boldsymbol{r}_0) = \frac{1}{16\pi}[(x-x_0)^2 + (y-y_0)^2] \ln \frac{(x-x_0)^2 + (y+y_0)^2}{(x-x_0)^2 + (y-y_0)^2} - \frac{y y_0}{4\pi}, \tag{3.2}$$

where $\boldsymbol{r} = (x, y)$ and $\boldsymbol{r}_0 = (x_0, y_0)$. With this choice, $G = \partial G/\partial y = 0$ on $y = 0$.

When the asymptotic approximation $\psi_{-\infty}$ found in the previous section is substituted for ψ in (3.1) the contribution from $x = -x_-$ vanishes for $x_- \to \infty$. For $r_+ \to \infty$ we use the boundary condition $\psi = O(r)$ and assume that, correspondingly, the order of magnitude of $\partial\psi/\partial N$, $\Delta\psi$, and $\partial\Delta\psi/\partial N$ are $O(r^{-1})$, $O(r^{-2})$, and $O(r^{-3})$ respectively. Then the contribution from the arc $r = r_+$ also vanishes in the limit $r_+ \to \infty$. Thus we may replace $\partial\Omega$ in (3.1) by the entire x-axis and the surface contour C. On the x-axis, the first two terms in the integrand vanish since $G = \partial G/\partial y = 0$, and $\partial\psi/\partial N$ and ψ are known from the boundary conditions in (2.7). Therefore, the integral along $y = 0$ can be evaluated analytically to be $-1-\gamma+\gamma y_0$. By means of the boundary conditions the integral along C can be rewritten so that $\partial\psi/\partial N$ becomes

the only unknown in the integrand. To do so we first use (2.6) and (2.8) in the first term in the integrand and integrate by parts twice. We thereby get:

$$\int_C \frac{\partial \Delta\psi}{\partial N} G\,\mathrm{d}s = \int_C \left[\frac{\partial p}{\partial s} - 3(T_x - \alpha T_y)\right] G\,\mathrm{d}s,$$

$$= \int_C \left[-2\frac{\partial^2 G}{\partial s^2}\frac{\partial \psi}{\partial N} + \beta\kappa\frac{\partial G}{\partial s} - 3(T_x - \alpha T_y)\,G\right]\mathrm{d}s, \tag{3.3}$$

where T_x and T_y are the components of the unit tangent vector to C. The end-point contributions vanish, since p, $\partial G/\partial x$, and $\partial G/\partial y$ go to zero while $\partial\psi/\partial N$ and G are bounded at both ends of C. The second term in the integrand is expressed in terms of $\partial\psi/\partial N$ by means of the second boundary condition in (2.8). Finally, the last term in the integrand in (3.1) vanishes, since $\psi = 0$ on C. Collecting these results and applying the left-hand formula in (2.3) we may therefore write (3.1) as

$$\psi(\boldsymbol{r}_0) = -1 - \gamma + \gamma y_0 + \int_C \left\{\left[\frac{\partial^2 G}{\partial N^2} - \frac{\partial^2 G}{\partial T^2}\right] v(s) + \beta\kappa\frac{\partial G}{\partial s} - 3(T_x - \alpha T_y)\,G\right\}\mathrm{d}s, \tag{3.4}$$

where $v(s) = \partial\psi/\partial N$ is the flow velocity in the surface.

From (3.4) we derive an integral equation by forming the derivative of the two sides in the direction of $\boldsymbol{N}'$, which is the outward unit normal vector to C at the point $\boldsymbol{r}'$. When, thereafter, we let $\boldsymbol{r}_0$ approach $\boldsymbol{r}'$ we obtain the equation

$$\tfrac{1}{2}v(s') = f(s') + \int_C \frac{\partial}{\partial N'}\left[\frac{\partial^2 G}{\partial N^2} - \frac{\partial^2 G}{\partial T^2}\right] v(s)\,\mathrm{d}s, \tag{3.5}$$

where

$$f(s') = \gamma N_y(s') + \int_C \left[\beta\kappa\frac{\partial}{\partial N'}\left(\frac{\partial G}{\partial s}\right) - 3(T_x - \alpha T_y)\frac{\partial G}{\partial N'}\right]\mathrm{d}s. \tag{3.6}$$

Since $\psi = 0$ on C, the right-hand side of (3.4) vanishes for points $\boldsymbol{r}_0$ on C, if the surface velocity determined by (3.5) is inserted in (3.4). On the other hand, if the integrals in (3.4) and (3.5) are taken along a curve C' different from C, the solution to (3.5) is not, in general, equal to the velocity component along C', and the right-hand side of (3.4), with this solution inserted, does not, in general, vanish. Therefore, we solve our problem by adjusting the curve of integration in (3.4) and (3.5) until the right-hand side of (3.4) vanishes when the corresponding solution to (3.5) is inserted. When this is achieved, the curve of integration is the surface contour, C, and the solution to (3.5) is equal to the surface velocity.

We start the iteration procedure, by means of which C is found, from an initial curve C_0 chosen in accordance with the known asymptotic properties of the surface. Thus, for $x < x_1$ and for $r = (x^2 + y^2)^{\frac{1}{2}} > r_N$, where x_1 and r_N are suitably chosen constants, C_0 coincides with the asymptotes $y = 1$ and $x = y\tan\vartheta_0$ respectively. On the part of C_0 between the points P_1 at $(x_1, 1)$ and P_N at $r_N(\sin\vartheta_0, \cos\vartheta_0)$ we choose $N-2$ collocation points, $P_2, P_3, \ldots, P_{N-1}$. In the iterative procedure these $N-2$ points are allowed to move along the corresponding normals to C_0, while the iterated curves all coincide with C_0 outside the interval between P_1 and P_N. Inside this interval the curves are approximated by a set of parabolas of which the one through P_i has the same tangent and curvature as the circle through P_{i-1}, P_i, and P_{i+1}. On the asymptote $y = 1$ the unknown v in (3.5) is replaced by the asymptotic value, $\frac{3}{2}+\gamma$, of the surface velocity. On the asymptote $x = y\tan\vartheta_0$ v is replaced by the function

$$\gamma\frac{2\cos\vartheta_0 - (\pi - 2\vartheta_0)\sin\vartheta_0}{\sin 2\vartheta_0 - \pi + 2\vartheta_0} + \frac{1+\gamma}{r}\frac{2\cos 2\vartheta_0 + 2}{(\pi - 2\vartheta_0)\cos 2\vartheta_0 + \sin 2\vartheta_0}. \tag{3.7}$$

This function was chosen for the following reason. Far out in the pool the flow field consists of two contributions. One of these is equal to the field in a fluid wedge with dihedral angle ϑ_0, which is bounded by a moving wall and a free surface. The other one is caused by the fluid flux from the film. An asymptotic representation of the first contribution, valid far away from the vertex, was determined by Moffatt (1964). The corresponding stream function is of the form

$$rf(\vartheta) = r(A\cos\vartheta + B\sin\vartheta + C\vartheta\cos\vartheta + D\vartheta\sin\vartheta), \tag{3.8}$$

where the angle ϑ is defined in figure 1. Since the flux from the film is independent of r, the second contribution can be derived from a stream function of the form

$$g(\vartheta) = A + B\vartheta + C\cos 2\vartheta + D\sin 2\vartheta. \tag{3.9}$$

When the sum $rf(\vartheta)+g(\vartheta)$ is inserted in the boundary conditions in (2.7) and (2.8), which are applied at $\vartheta = -\vartheta_0$ and $\vartheta = 0$ respectively, f and g can be found. The function in (3.7) is the corresponding surface velocity. Between P_1 and P_N, v is expressed as a continuous function given by polynomials of degree one between consecutive points $P_1, P_2, \ldots, P_N$. The value of the function at P_i is denoted by v_i.

Introducing the approximations described above and requiring the integral equation to be satisfied at the collocation points we obtain a set of linear algebraic equations with unknowns $v_2, \ldots, v_{N-1}$ and coefficients depending on the shifts $t_2, \ldots, t_{N-1}$ of the collocation points along the normals of C_0. The function found by solving the system is inserted in (3.4) whose right-hand side is evaluated at the collocation points. By means of a method developed by Madsen (1975), and implemented in the subroutine VG02AD of the Harwell subroutine library, the surface is finally found by minimizing $\epsilon \equiv \max_i |\psi_i|$, where $\psi_i = \psi_i(t_2, \ldots, t_{N-1})$ denotes the value of the right-hand side of (3.4) at P_i.

In the numerical calculations, x_1 and r_N were chosen so that the surface was close to the asymptotes and v_i close to the asymptotic expressions at the first and the last several collocation points. In order that this was achieved at the upper end, x_1 had to be -30, when β was large, and -15 for $\beta = 0$. In the pool, the asymptotic values are approached much slower so that, while $r_N = 70$ was a typical value, r_N had in some cases to be increased to several hundreds. However, since v varies very slowly for large r, the number of collocation points then only had to be increased by a few. For each ϑ_0 considered, only a few trials were needed in order to find an initial curve, C_0, consisting of a part of each asymptote and a connecting circular arc, so that the iteration procedure converged. Starting from the solution for $\beta = \gamma = 0$ and stepping through intervals of β and γ we could then obtain all the other results presented in the next section. While stepping through the parameter intervals we kept N relatively small, $N = 25$ being a typical value. For the sets of parameters, which were selected for presentation, the calculations were repeated once or more with N being increased until a further increase of N did not change the surface profile. The largest value used for N was 50. Apart from one exception to be mentioned later ϵ was 10^{-6} or less. The computations were carried out on the IBM 3081 computer at the Lyngby branch of the Danish University Computing Centre. As an example of the computing times we mention that with the surface profile for $\vartheta_0 = 0$, $\beta = 200$, and $\gamma = 0$ as the starting approximation and $N = 28$, the iteration procedure for obtaining the curve for $\vartheta_0 = 0$, $\beta = 210$, and $\gamma = 0$ required 50 s CPU time. This time could be reduced considerably since in the program the same matrix elements were computed several times, but it was decided that the intended use of the program did not warrant systematic attempts to minimize the computing time.

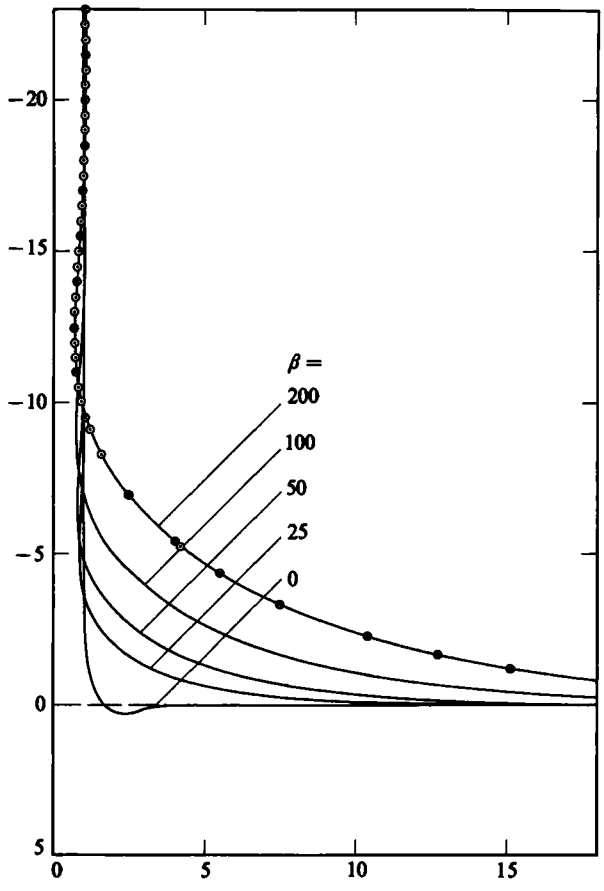

FIGURE 2. Surface profiles for $\vartheta_0 = 0°$, $\gamma = 0$, and $\beta = 0$, 25, 50, 100, and 200. The locations of the collocation points for $\beta = 200$ are indicated by circles ($N = 50$) and crosses ($N = 28$).

4. Results and discussion

By means of the method described in the preceding section we have determined the surface profile and surface velocity for several sets of values of the parameters ϑ_0, β, and γ. We now present and discuss some of these results.

Figure 2 shows the surface profile for $\gamma = \vartheta_0 = 0$ (a fixed, vertical wall) and β ranging from 0 (no surface tension) to 200. In order to indicate the accuracy of the results we have shown the positions of the collocation points for $\beta = 200$ and $N = 28$ or 50 respectively. It is seen that within drawing accuracy the two sets of points fit nicely onto the same curve. A comparison between the curves for different values of β shows that for larger surface tension the surface rises in a smoother curve so that the surface area is reduced. Another feature, whose explanation is less obvious, is the thinning of the film just above the point where the surface starts to curve away from the wall. It is this feature which has previously been studied and explained by Ruschak (1978). Briefly, his explanation can be put as follows. On the curved part of the surface, between the almost plane film and pool surfaces, the pressure is negative because of the surface tension. Consequently, there is a downward pressure gradient in the fluid at the top end of the curved surface. However, since the flow is Stokesian, the forces acting on any part of the fluid must be in equilibrium. This

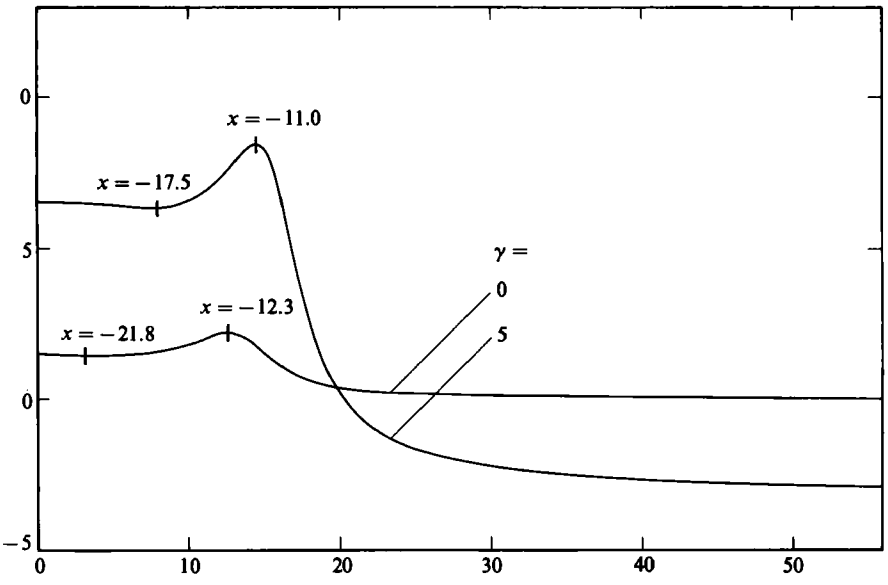

FIGURE 3. Velocity distributions along the surface for $\vartheta_0 = 0°$, $\beta = 200$, and $\gamma = 0$ and 5. Arc lengths are measured from the points where $x = -25$. The locations (x-values) of the extrema are indicated at the curves.

is achieved by the thinning of the film in that region. Thereby the average velocity and, hence, the velocity gradient across the film are increased, so that the upward shear force from the wall exceeds the gravity forces enough to balance the downward pressure force.

The results presented in figure 2 extend those found in Ruschak (1978) to smaller values of the surface tension. They agree with Ruschak's theory in that the thinning becomes less and less pronounced as β decreases and disappears when β vanishes.

For $\beta = 200$ and $\vartheta_0 = \gamma = 0$ the surface velocity is shown in figure 3 as a function of the arc length. These results may serve as a partial check on the solution. It is seen that the velocity does indeed approach the asymptotic values 1.5 and 0 for $x \to -\infty$ and $y \to \infty$ respectively, and that it assumes a maximum value at the point of smallest thickness. By interpolation between the nearest collocation point we find that the extremum is located at $x = -12.3$, and that the film thickness is 0.679 and the surface velocity is 2.187 at this point. If the film thickness along the wall is assumed to be $h = h(x)$ rather than unity, and the usual approximations of lubrication theory are used, the velocity distribution is found to be

$$v(y) = \frac{3}{2h^3}(1+\gamma(1-h))(2h-y)y+\gamma, \tag{4.1}$$

if $\vartheta_0 = 0$. For $\gamma = 0$ and $h = 0.679$ the surface velocity computed from (4.1) is 2.209, which agrees nicely with the above value. The figure also shows that at $x = -21.8$ there is a local minimum of the velocity and a corresponding local maximum of the film thickness. Because of the scale used in figure 2 this maximum is, however, barely visible. Ruschak ascribes the presence of this thickening, too, to the mechanism described above. Similar maxima in thickness, which are too weak to be seen in the graphical presentation in figure 2, are found in the numerical results for $\beta = 100$, 50 and 25. For those of the β-values, for which the collocation points were distributed

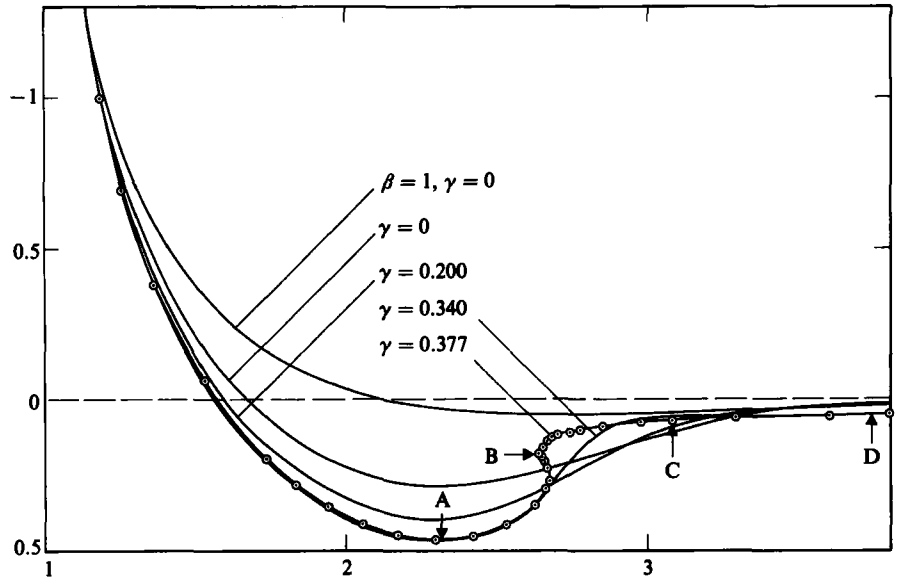

FIGURE 4. Surface profiles for $\vartheta_0 = 0°$, $\beta = 0$, and $\gamma = 0$, 0.2, 0.34, and 0.377, and for $\vartheta_0 = 0°$, $\beta = 1$, and $\gamma = 0$. The locations of the collocation points for $\gamma = 0.377$ are indicated by circles. Corresponding points on the profile for $\gamma = 0.377$ and the velocity distribution in figure 5 are shown by letters A, B, C, and D.

far enough up on the film, a second minimum, still weaker than the first two extrema, was also found.

Wilson & Jones derived an asymptotic formula for the minimum film thickness which reads in our notation: $h_{\min} \sim 1.27/\beta^{\frac{1}{15}}$. According to this formula $h_{\min} \sim 0.80$ and 0.75 for $\beta = 100$ and 200, respectively, while the corresponding values found by the present method are 0.733 and 0.679. In view of the fact that these β-values could not be expected to be within the realm of validity of the asymptotic theory, the agreement seems quite good.

A rather interesting feature of the surface profiles in figure 2 is the depression of the pool surface for $\beta = 0$. A larger scale plot of the surface profile around the depression is found in figure 4. If inertial forces were important, such a depression would hardly be surprising, but since they are neglected in Stokes approximation another explanation of the depression is needed. We propose the following one. As the fluid leaves the film, the streamlines fan out, so that the direction of the fluid velocity turns downwards with increasing depth. Although the speed decreases in downward direction so that, eventually, the vertical component, v_x, of the velocity vanishes, there is an interval just below the surface where v_x is increasing. Therefore, the normal derivative of the normal velocity component at the surface, $\partial v_N/\partial N$, is positive, and the boundary condition $p = 2\,\partial v_N/\partial N$ then requires the pressure, too, to be positive. In the almost stagnant fluid far out in the pool the pressure increases in the downward direction, and it seems unlikely that the dynamic forces in the fluid are strong enough to reverse the direction of the vertical pressure gradient at points in the pool which are closer to the wall. Thus, in order that the pressure may be positive at the surface, the surface must be lower than at infinity.

Our numerical results for the surface velocity, v, found by solving the integral equation allow us to quantify to some extent the above argument. For

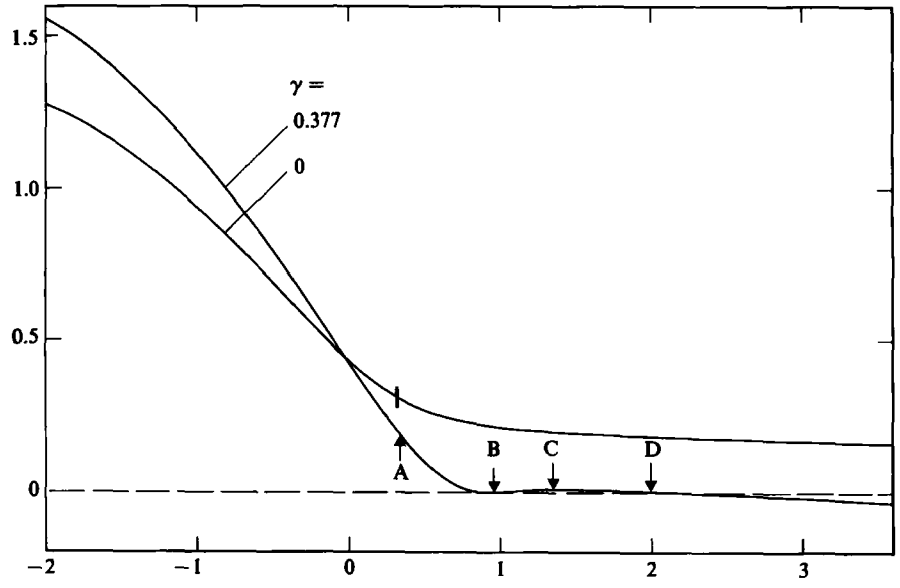

FIGURE 5. Velocity distribution along the surface for $\vartheta_0 = 0°$, $\beta = 0$, and $\gamma = 0$ and 0.377. Arc lengths are measured from the points where $y = 2$. The point corresponding to the bottom of the depression for $\gamma = 0$ is indicated by a vertical bar.

$\vartheta_0 = \beta = \gamma = 0$ the surface velocity is shown as a function of the arc length, s, in figure 5. The point corresponding to the bottom of the depression is indicated in the graph, and it is seen that $\mathrm{d}v/\mathrm{d}s$ is negative there. From the numerical results we find that $\mathrm{d}v/\mathrm{d}s = -0.297$. From the boundary condition $p = 2\,\partial v_N/\partial N$ and the continuity equation it then follows that the pressure at the bottom of the depression is $p_\mathrm{d} = -2\mathrm{d}v/\mathrm{d}s = 0.594$. The left-hand equation in (2.6) shows that, at the same level as the bottom of the depression, $x = x_\mathrm{d} = 0.286$, the pressure at infinity is $p_\infty = 3x_\mathrm{d} = 0.858$. So, there exists a pressure difference $p_\infty - p_\mathrm{d} = 0.264$ between infinity and the bottom of the depression, but the dynamic forces are strong enough to account for a difference of this size. Thus, integrating the equation to the right in (2.6), which may be written, $p_y = \Delta v_y$ for $\vartheta_0 = 0$, along the line $x = x_\mathrm{d}$ from the bottom of the depression at $y = y_\mathrm{d} = 2.32$ to infinity we get

$$p_\infty - p_\mathrm{d} = \int_{y_\mathrm{d}}^{\infty} \frac{\partial^2 v_y}{\partial x^2}\,\mathrm{d}y - \left(\frac{\partial v_y}{\partial y}\right)_{y=y_\mathrm{d}}. \tag{4.2}$$

Since $\partial v_y/\partial y = 0$ at infinity. The first term on the right-hand side of (4.2) is difficult to estimate, but the second one can again be evaluated from the data of the surface velocity, since $-\partial v_y/\partial y = -\mathrm{d}v/\mathrm{d}s = 0.297$ at the bottom of the depression. Thus this term is a little larger than the pressure difference. Consequently, the integral in (4.2) must be negative, which is reasonable, because v_y is decreasing in the downward direction, and $\partial v_y/\partial x = 0$ everywhere in the plane pool surface so that $\partial^2 v_y/\partial x^2$ must be negative at least in the plane surface itself.

Figure 4 also shows that if β is increased to 1 the depression is much more shallow, but it should still be detectable in an experiment. Based on the following data for glycerine at 20 °C, which are given in (Weast 1982): $\rho = 1.2613$ g/cm^3, $\sigma = 63.4$ dynes/cm, and $\mu = 14.90$ g cm^{-1} s^{-1}, the value $\beta = 1$ is obtained if the film

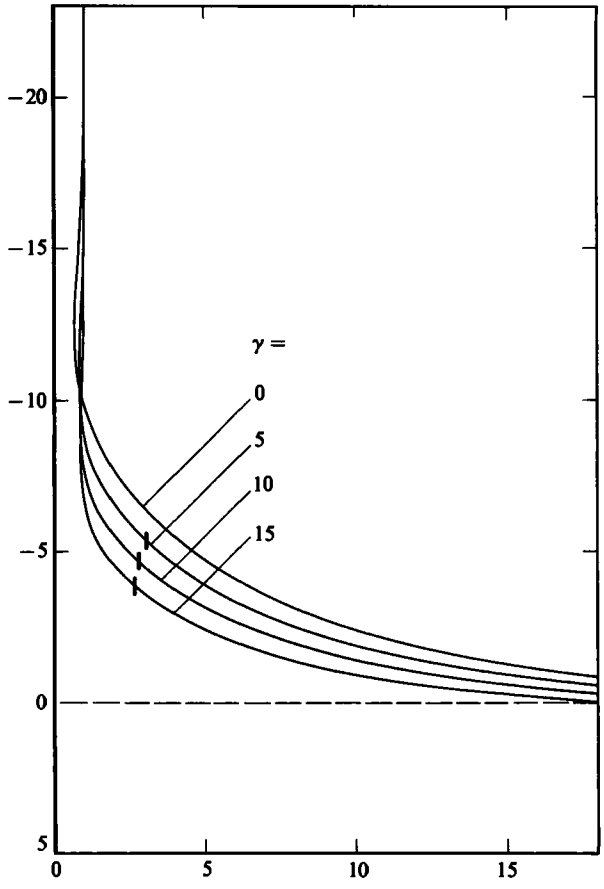

FIGURE 6. Surface profiles for $\vartheta_0 = 0°$, $\beta = 200$, and $\gamma = 0$, 5, 10, and 15. For $\gamma > 0$ the stagnation points are indicated by vertical bars.

thickness $h_0 = 0.39$ cm. The corresponding Reynold's number based on the film thickness and the surface velocity at infinity is 0.21.

We now turn to the case of a wall moving downwards ($\gamma > 0$). As mentioned in the introduction this case was investigated by Wilson & Jones (1983) in the limit of large surface tension. In their analysis they had to introduce a further limitation which, in our notation, is expressed by the requirement that γ/β must be small, and they found no solutions exhibiting a depression of the surface. Since the formation of a depression requires the surface area to be increased, it is to be expected that if β is large, a depression can only be created if the wall velocity is large too. Indeed, as the results in figure 6 for $\beta = 200$ show, even if the wall velocity is as large as 15 times the average of the fluid velocity relative to the wall, the surface elevation is only reduced to about 50 % of the corresponding one for a wall at rest.

When $\gamma > 0$ a circulating motion in the counterclockwise direction is set up in the pool, so that the surface velocity, v, approaches a negative value for $y \to \infty$. Since $v > 0$ near the wall, a stagnation point must exist somewhere in between. The locations of the stagnation points are indicated on the curves in figure 6. Figure 3 includes a graph of the surface velocity as a function of arc length for $\vartheta_0 = 0$, $\beta = 200$, and $\gamma = 5$. The velocity varies between the limits $\gamma + \frac{3}{2} = 6.5$ for $x \to -\infty$

and $-2\gamma/\pi = -3.18$ for $y \to +\infty$. At $x = -11.0$ the film takes its smallest thickness of 0.826 and the velocity reaches its maximum value of 8.33. At $x = -17.5$ the film thickness has a local maximum of 1.019 and the velocity has a local minimum of 6.34. These values compare well with those found from formula (4.1). Thus, for $\gamma = 5$, (4.1) gives the values $v(h) = 8.40$ for $h = 0.826$ and $v(h) = 6.33$ for $h = 1.019$. In figure 3 it is worth noting that the asymptotic velocity value in the pool is approached much slower for $\gamma = 5$ than for $\gamma = 0$. Therefore, it was necessary in the computations to push the point, P_N, beyond which the surface is replaced by its asymptote and the velocity by its asymptotic approximation, much further out for $\gamma = 5$ than for $\gamma = 0$. As a consequence, the computational work became much larger.

Returning again to figure 6 we note that for a fixed β at 200 the thinning of the film becomes less and less pronounced as γ is increased. This can also be explained along the lines of Ruschak's theory in connection with formula (4.1) from which the non-dimensional shear force per unit area of the wall is found to be $v'(0) = 3(1+\gamma(1-h))/h^2$. If $h = 1$, this force balances the gravity force on the fluid, which is $3h$ per unit area of the wall. If we put $h = 1-\Delta$ and assume that $\Delta \ll 1$, the upward resultant of the two forces per unit area is approximately equal to $F \equiv 3(3+\gamma)\Delta$. Therefore, if a given downward pressure force is to be balanced by F, the necessary value of Δ is smaller the larger the value of γ.

For $\beta = 0$ the influence of the wall motion on the surface profile is considerable. This is demonstrated in figure 4. To begin with, the changes from the profile for $\gamma = 0$ are only quantitative. Thus, in the profile for $\gamma = 0.2$, which is typical for this interval, the depression is of the same general shape as that of $\gamma = 0$, only deeper, and this development continues as γ increases to about 0.34. In the further, short γ-range, through which we have been able to continue the computations, appreciable changes occur only on the outer slope of the depression, which becomes steeper with a vertical part appearing when γ is about 0.370, and eventually a projection starts to develop. It is tempting to imagine that this projection will continue to grow as γ increases further, but we have not been able to obtain reliable results for γ larger than 0.377. In order to substantiate the result for the surface profile for $\gamma = 0.377$ we have chosen to show the location of the collocation points rather than just the curve through them. As is seen, in order to be able to reproduce the rather complicated shape around the projection it was necessary to concentrate many of the 50 collocation points which were used in that neighbourhood. Even then it was not possible to reduce the error ϵ below 8×10^{-5} as compared to the values 10^{-6} or less which could easily be prescribed in other cases. When we attempted to consider larger values of γ the smallest ϵ-values for which convergence could be achieved increased rapidly and the corresponding distributions of the collocation points started to become erratic.

In figure 5 the surface velocity for $\gamma = 0.377$ is shown as a function of the arc length. In order to facilitate the comparison with the surface profile in figure 4 a number of corresponding points on the two curves are indicated. It is seen that as the depression is passed, the velocity drops to a local, positive minimum value almost at the salient point (B) of the projection, and that beyond that point the velocity stays very small (with a local maximum in C) until the stagnation point (D) is reached. Thereafter the velocity approaches monotonously the limiting value $-2\gamma/\pi = -0.240$ at infinity.

As examples of results for tilted walls we present some for $\vartheta_0 = 45°$. Figure 7 shows the surface profile for $\beta = 300$. Since β is inversely proportional to $\cos\vartheta_0$, this value corresponds approximately to the same values of σ, ρ, μ, and h_0 as does $\beta = 200$ for

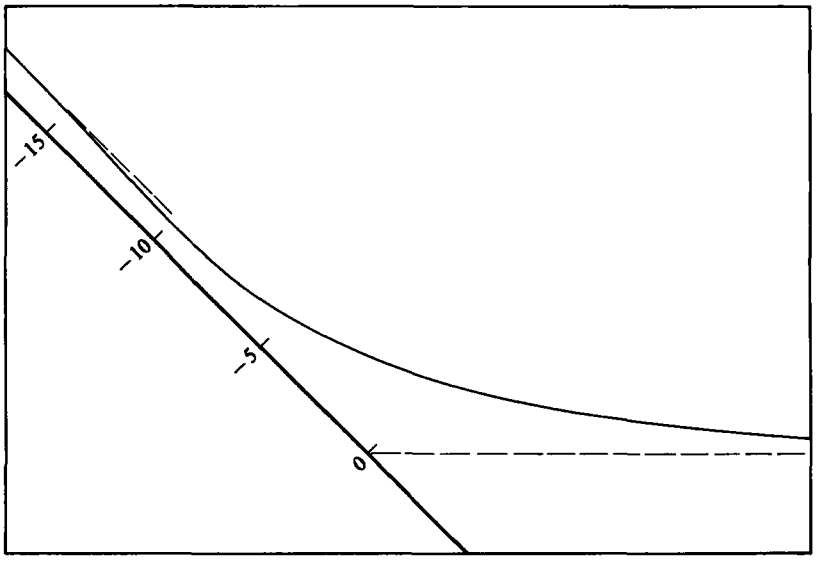

FIGURE 7. Surface profiles for $\vartheta_0 = 45°$, $\beta = 300$, and $\gamma = 0$. The asymptotes $y = 1$ and $y = x$ are shown as broken lines.

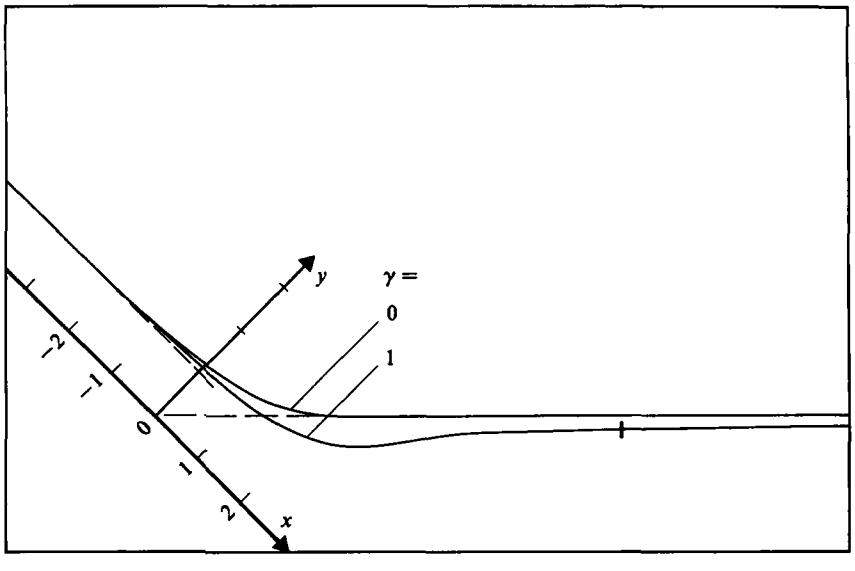

FIGURE 8. Surface profiles for $\vartheta_0 = 45°$, $\beta = 0$, and $\gamma = 0$ and 1. The asymptotes $y = 1$ and $y = x$ are shown as broken lines. For $\gamma = 1$ the stagnation point is indicated by a vertical bar.

$\vartheta_0 = 0$. A comparison with figure 2 shows that the surface curvature just below the film is larger when $\vartheta_0 = 0°$ and $\beta = 200$, than when $\vartheta_0 = 45°$ and $\beta = 300$. Consequently, the vertical pressure gradient in the lowest part of the film is larger in the first case. According to Ruschak's theory, the reduction in film thickness should then be larger, too. As the figures show, this is indeed the case. The computed minimum thicknesses are 0.679 for $\vartheta_0 = 0°$ and $\beta = 200$ and 0.784 for $\vartheta_0 = 45°$ and $\beta = 300$.

Figure 8 shows the profiles for $\beta = 0$ and $\gamma = 0$ and 1. For $\gamma = 0$ there is a

depression in the surface, but since its depth is only 0.02 it is almost invisible in the graph. For $\vartheta_0 = 45°$ the value of the derivative $\partial v_N/\partial N = -\mathrm{d}v/\mathrm{d}s$ at the bottom of the depression is only 0.16 so that the pressure at the same point is $p = 2\,\partial v_N/\partial N = 0.32$. Since the depression is almost non-existent, such a pressure is apparently small enough to be balanced by the pressure difference between the depression and infinity which is set up by the dynamic forces.

For $\vartheta_0 = 45°$ the shear stress produced by the wall motion is not perpendicular to the surface. Consequently, the resulting change of the surface profile is smaller than if $\vartheta_0 = 0°$, and we were able to get convergent results for γ up to and including $\gamma = 1$.

However, as will be noted, for $\vartheta_0 = 45°$ the influence of the wall motion stretches far out. Indeed, even for $x \approx y \approx 200$ the surface is still almost at the distance 0.1 from the asymptote $x = y$. The results for this case also differed from all those for $\vartheta_0 = 0°$ and γ positive in that the distance, r_N, from where the surface velocity is put equal to the asymptotic approximation had to be increased to 250 before the values of the velocity at the outermost collocation points were reasonably close to the asymptotic values. For $\vartheta_0 = 0°$ the approach to the asymptotic values is much faster. A possible explanation of this fact is that, as shown by Moffatt (1964), in a fluid wedge bounded by a moving wall and a free surface and with a dihedral angle less than about 78° (i.e. with ϑ_0 larger than about 12°), the biharmonic equation admits solutions corresponding to a system of eddies. So it is likely that the flux from the film generates such a flow in the pool. Although the eddies are damped with increasing distance from the film they will enlarge the interval which must be traversed before the asymptotic flow field dominates completely.

The present work was initiated while the author was a guest at the Department of Mathematics, Stanford University. The author wishes to express his sincere gratitude to Julie Damms Studiefond for financial support and to Professor Joseph B. Keller for his hospitality during the stay. Thanks are also due to Drs P. S. Larsen and D. H. Peregrine for discussions of the results and to Dr K. Madsen for advice on the use of his optimization method.

REFERENCES

Cook, R. A. & Clark, R. H. 1973 *Ind. Engng Chem. Fundam.* **12**, 106–114.

Hansen, E. B. 1985 *Free Boundary Problems: Applications and Theory* (ed. A. Bossavit, A. Damlamian & M. Fremont), vol. 4, pp. 391–394. Pitman.

Kelmanson, M. A. 1983 *J. Engng Maths* **17**, 329–343.

Madsen, K. 1975 *Math. Prog. Stud.* **3**, 110–126.

Moffatt, H. K. 1964 *J. Fluid Mech.* **18**, 1–18.

Ruschak, K. J. 1978 *AIChE J.* **24**, 705–709.

Ruschak, K. J. 1985 *Ann. Rev. Fluid Mech.* **17**, 65–89.

Weast, R. C. (ed.) 1982 *CRC Handbook of Chemistry and Physics*, 62nd edn, pp. C312, F38, F46. CRC Press.

Wilson, S. D. R. & Jones, A. F. 1983 *J. Fluid Mech.* **128**, 219–230.